

phys. stat. sol. (a) **150**, 613 (1995)

Subject classification: 61.16 and 68.35; S9.12

*Max-Planck-Institut für Mikrostrukturphysik, Halle/Saale<sup>1)</sup> (a) and  
Fachbereich Physik der Freien Universität Berlin<sup>2)</sup> (b)*

## Scanning Electron Microscopical Inspection of Uncoated CaF<sub>2</sub> Single Crystals

By

H. JOHANSEN (a), S. GOGOLL (b), E. STENZEL (b), and M. REICHLING (b)

(Received June 12, 1995)

Dedicated to Professor Dr. JOHANNES HEYDENREICH on the occasion of his 65th birthday

Cleaved and mechanically polished surfaces of CaF<sub>2</sub> single crystals in the uncoated state are investigated by means of secondary (SE) and backscattered (BE) electron imaging in the scanning electron microscope with respect to their strongly different charge-up properties. There is a relationship between the density of preparation-induced defects and the amount of surface charge detectable by characteristic image disturbances. Different electrical contacting techniques of the crystals are tested to obtain imaging free of charge. For the cleavage face the relatively low electrical resistance of the bulk material of  $\rho \approx 10^{13} \Omega \text{ cm}$  controls the imaging conditions rather than the electron trapping by cleavage-induced surface defects. On mechanically polished surfaces already during the first slow scan with  $E_p < 5 \text{ keV}$  an equipotential surface is formed leading to a pronounced electron mirror effect detectable by SE and BE. However, also in this case imaging of selected crystal areas free of disturbances succeeds if they are located within an electrical deceleration field.

Spaltflächen und mechanisch polierte Oberflächen von CaF<sub>2</sub>-Einkristallen werden im unbedampften Zustand mit Sekundärelektronen (SE) und Rückstreuielektronen (RE) hinsichtlich ihrer sehr unterschiedlichen Aufladungseigenschaften in einem Rasterelektronenmikroskop untersucht. Es besteht eine Beziehung zwischen der Dichte präparationsinduzierter Defekte und dem Grad der durch charakteristische Bildstörungen erfassbaren Oberflächenaufladung. Für eine Abbildung frei von beobachtbaren Aufladungen werden verschiedene elektrische Kontaktierungen der Kristalle erprobt. Die Abbildungsverhältnisse an einer Spaltfläche sind eher durch die elektrische Volumenleitfähigkeit des Materials ( $\rho \approx 10^{13} \Omega \text{ cm}$ ) als durch den Elektroneneinfang an spaltungsinduzierten Oberflächendefekten bestimmt. Auf mechanisch polierten Oberflächen bildet sich bereits während des ersten Bilddurchlaufes und für  $E_p < 5 \text{ keV}$  eine Äquipotentialfläche aus, die zu einem ausgeprägten Elektronenspiegel-Effekt führt, der mit SE und RE erfaßt werden kann. Jedoch auch in diesem Fall gelingt eine störungsfreie Abbildung ausgewählter Kristallbereiche, wenn sich diese in einem elektrischen Verzögerungsfeld befinden.

### 1. Introduction

Charging insulating areas of solids during investigation by electron probe techniques is usually unwanted because of resulting artifacts. Especially in the SE imaging mode of SEM using a large frame time, charging of solid surfaces does not only cause a SE trajectory-related loss of detection but also direct beam broadening and beam deflection of the primary electrons. Measuring the image shift can be used to estimate the amount of charge stored on the dielectric surface [1]. The indefinite storage of surface charges at moderate temperatures is a significant characteristic of insulators [2], since it indicates trapping of the injected carriers

<sup>1)</sup> Weinberg 2, D-06120 Halle/Saale, Federal Republic of Germany.

<sup>2)</sup> Arnimallee 14, D-14195 Berlin, Federal Republic of Germany.

at pre-existing defects or at defects which are introduced by surface modification as, for example, polishing, cleavage, or irradiation by electrons or photons. All these treatments can result in various degrees of near-surface deformation which is known to be accompanied by the generation of different densities and distributions of point defects [3]. To study the relation between structural modifications of the material surface and the electron dose-dependent surface potential, charge-up of dielectrics has also intentionally been generated (SEM mirror effect [4]).

Surface charge generation and neutralization have been demonstrated to be a result of recombination processes involving localized levels in the band gap of the insulator [5]. Due to the localization of injected electrons and secondary emission as well as defects produced during electron irradiation, the sign of the trapped charge and the resulting macroscopic surface potential may locally change between positive and negative. All these factors can sensitively influence SEM imaging conditions so that contrast interpretation cannot be generalized in most cases. Here, one has carefully to distinguish between the electron beam *induced* charge and the *detection sensitivity of charge* given by characteristic (SE) image disturbances. Therefore, no sharp criterion to define the dielectric surface state "free of charge", for example, by measuring the shift of the energy spectrum of SE [6] can be stated from solely SEM *imaging* investigations. Only image disturbances indicated by sudden jumps of the signal intensity between neighbouring scanning lines, the characteristic vanishing of topographic surface structures by local high or low SE yields, or the generation of the electron mirror effect can be related to beginning charge-up of insulators.

A lot of experimental investigations with respect to beam voltage, frame time, and crystal contacting to ground are necessary to reliably characterize the charge behaviour of an uncoated insulating material. This is also of great importance for the quantitative microanalysis of dielectrics by Auger electrons. Furthermore, the interpretation of charge phenomena of insulators is particularly difficult since often most of the available parameters for the dielectric are related to the *bulk* of the material and not to the surface (dielectric constant  $\epsilon$ , electrical resistivity  $\rho$ , for example).

The aim of this paper is the description and interpretation of controlled SEM charging and discharging experiments on uncoated cleaved and polished surfaces of the wide-band-gap material  $\text{CaF}_2$  representing the state of art in low contamination, high-quality IR and UV optical crystals. For a discussion of charging phenomena in alkaline earth fluorides it is important to know the effects of unavoidable impurities on their surface properties (mainly contamination by carbon, oxygen, or moisture). In  $\text{CaF}_2$  the influence of oxygen ions substituting fluorine results in an increasing electrical conductivity [7]. Early stages of decomposition of the material by the electron beam [8, 9] possibly influencing the electrical surface conductivity have been disregarded.

## 2. Experimental

SEM experiments were carried out on UV-grade  $\text{CaF}_2$  single crystals from K. Korth oHG, Kiel with one cleaved (111)-surface and one optically polished. The dimensions were  $20 \times 20 \text{ mm}^2$  with a thickness of 3 to 6 mm. Crystals were always stored in air so that SEM inspections were always made regarding unavoidable surface contamination. Both surfaces were topographically studied after applying various preparation techniques to ensure sufficient electric contact between the crystal surface and the metallic specimen stub (see Fig. 1). On the uncoated cleavage face only four conductive paint dots at the periphery of the crystal and corresponding conductive paths on the crystal sides have been applied

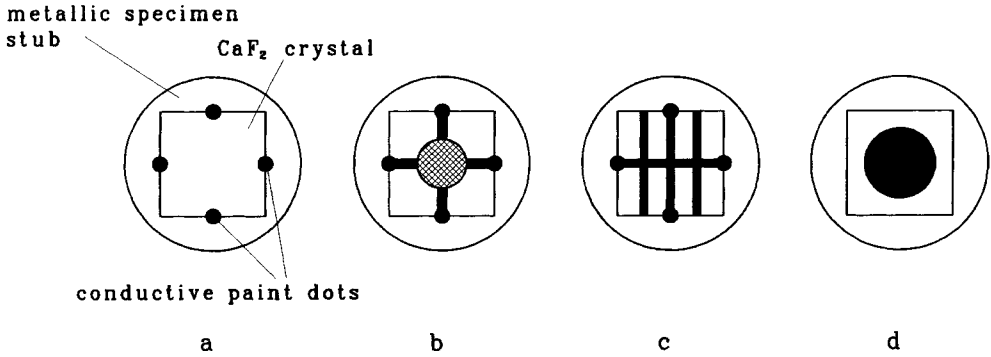


Fig. 1. Charge leakage paths to ground: scheme of different contacting modes of the large-area  $\text{CaF}_2$  crystals which were used to minimize charge-up (see text)

(Fig. 1a) forcing at least parts of the crystal surface to a definite potential. In a second experiment a copper mesh of 10 mm diameter containing quadratic openings of  $500 \times 500 \mu\text{m}^2$  was directly mounted on the crystal by small paint dots and grounded by conductive paint paths (Fig. 1b). A variation of the charge leakage of insulated areas of different sizes was realized by applying two grids which could be shifted against each other (see inset of Fig. 6). On the uncoated polished surface grounded conductive paths of 20 nm thickness have been prepared by carbon evaporation through a lithographic mask, which was directly mounted on the crystal surface (Fig. 1c). This results in a local electrical deceleration field on the dielectric surface between insulated areas and charge leakage during the scanning period of the electron beam. To study the onset of charging on the cleaved surface for constant probe current, beam energy, and frame time, as a function of magnification only, a single large-area conductive tab fixed at the crystal back side was used (Fig. 1d).

The studies were done with a field-emission SEM having an oil-free vacuum of  $10^{-5}$  Pa, enabling secondary electron imaging at primary electron energies as low as  $E_p = 0.5$  keV. No visible topographic modification of the surfaces was observed due to the electron probe–crystal interaction. All micrographs represent only reproducible charge phenomena.

### 3. Results and Discussion

#### 3.1 Charge characteristic of the uncoated cleaved surface

If large  $\text{CaF}_2$  crystals are electrically grounded only at the periphery (cf. Fig. 1a) topographical surface features as cleavage steps, small particles, or substructures on terraces are detectable nearly without image disturbances in the low voltage range up to  $E_p \approx 4$  keV. The onset of SE intensity jumps depends on the position of the scanned area relative to the position of the grounded conducting dots and clearly indicates the influence of the conducting path length to ground on the surface. A typical example from the centre of a crystal is shown in Fig. 2. Near the second cross-over energy of  $\text{CaF}_2$ ,  $E_2$  ( $\Phi = 0^\circ$ )  $\approx 1.8$  keV [10] no charge-up is observed. The image contrast of detached crystallites is solely topographically determined by shadowing and edge emission of SE.

Above a distinct sharp threshold value of the electron beam energy locally a “flat”, not topographically determined dark SE contrast on cleavage terraces can be observed (Fig. 3a, see arrows,  $E_p = 8$  keV). It reversibly appears and disappears during slow scan imaging

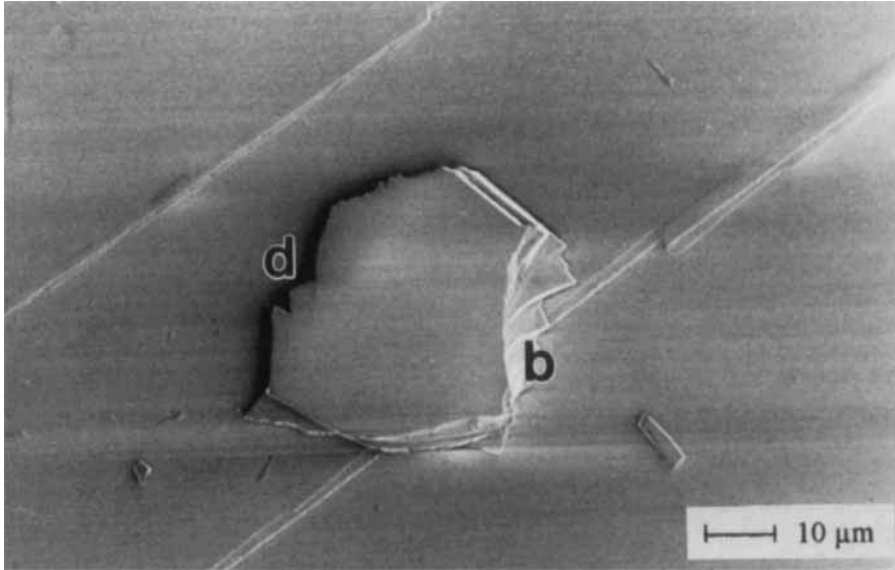


Fig. 2. Typical condition of secondary electron imaging of the centre of the cleavage face before onset of charge-up;  $E_p = 2$  keV ( $\Phi = 0^\circ$ ). The dark (d) and bright (b) contours of a detached crystallite after cleavage solely arise from the shadowing and edge effects of the SE yield, respectively

when varying the beam energy around the threshold value of  $E_{th} \approx 3.5$  keV in this case. The accompanied overall flicker noise of the intensity for  $E_p > E_{th}$  does not yet result in a loss of lateral resolution of steps and structural details of terraces. The cloud-like dark areas indicate possibly cleavage-induced defect centres which may be a result of locally enhanced recombination of beam-induced carriers on the uncoated insulator surface. Using the TV scan mode (Fig. 3b) with its strongly reduced dwell time of the electron probe which significantly lowers the effective charge input it is obvious that the SE signal overshoot from small crystallites in Fig. 3a has another physical nature than the defect centres marked by arrows in the same micrograph.

Usually, the interaction of the electron beam with an insulator results in patterns of the electric field of the trapped charges due to inherent defects [5] and there is experimental evidence for the inability to charge an ultra-pure ionic crystal even for incident energies as high as  $E_p = 5$  keV [11]. However, we believe that there is also a relation between the possibility to detect locally distributed SE yield variations due to (preparation-induced) trapping centres near the surface and the electrical (bulk) resistivity of the insulator. Since the latter is relatively low for  $\text{CaF}_2$  ( $\rho = 10^{13} \Omega \text{ cm}$  [12]) the simple specimen contacting of Fig. 1a enables an acceptable SE imaging of the cleaved surface which does not mask local effects of carrier recombination by image disturbances due to global charge-up. Furthermore, contrary to the centre of the crystal, at the periphery near the conductive paint dots even in the range of  $E_p > 15$  keV it is possible to detect fine cleavage steps free of charge, Fig. 4. This indicates the effect of increased charge loss by electric surface conduction of a dielectric crystal if the surface leakage paths to ground are shortened.

The superposition of the cleavage topography by local charge-up can be completely eliminated using the backscattered electron (BE) mode as demonstrated in Fig. 5a. Also

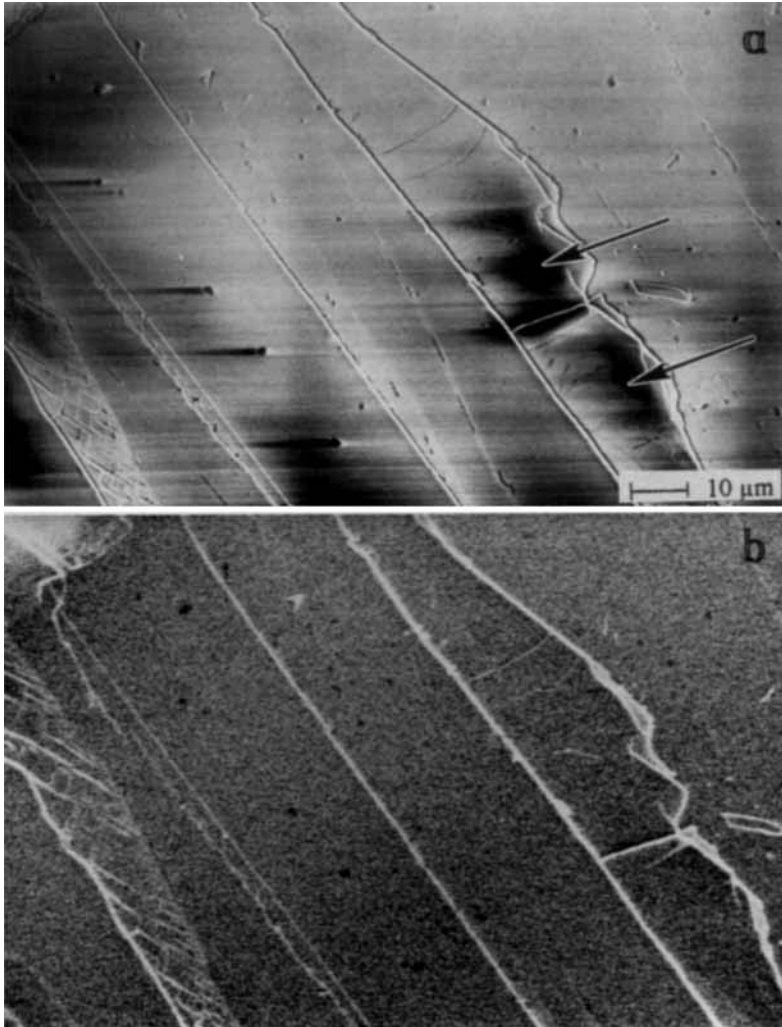


Fig. 3. a) Steps, terraces, and small crystallites can be detected weakly charged without loss of information on the uncoated cleavage face. b) Cloud-like distributed concentrations of recombination active defects (arrows in a) disappear in the TV scan mode; SE,  $E_p = 8 \text{ keV}$

during repeated slow scans no charge-up arises in the BE micrograph whereas the corresponding SE micrograph exhibits blurring (Fig. 5b). This may be due to the fact that the surface potential of the cleaved surface is only several hundred volts or less solely affecting the SE trajectories but not those for the BE. In spite of disturbances due to charge-up the SE micrograph enables one to detect local surface contamination by a weak contrast of decreased SE yield (see arrows Y in Fig. 5b) that cannot be observed in the BE mode. This surface-sensitive contrast formation of the uncoated cleaved surface has to be carefully distinguished from that of a small area tilt which is generally detectable by means of *both* signals, SE and BE (see arrow T).

It should be noted that the *surface charge* locally generated by the low-energy electron probe on the cleaved surface cannot have a significant disturbing effect. The time constant

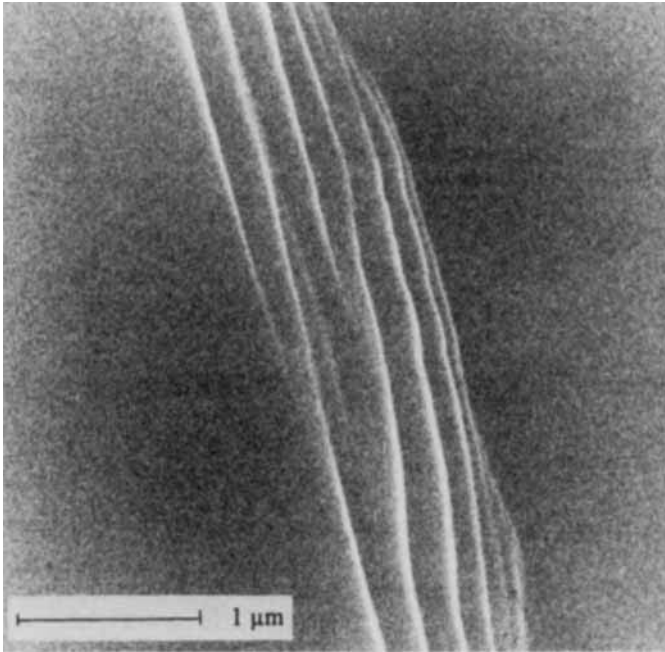


Fig. 4. High resolution SE micrograph of fine steps of the uncoated cleavage face detected free of charge from an area located near a conductive paint dot,  $E_p = 17$  keV

of the charge decay,  $\tau_0 = \epsilon_r \epsilon_0 \rho$  [13, 14] for  $\text{CaF}_2$  only amounts to  $\tau_0 \approx 7$  s ( $\epsilon_r \epsilon_0$  dielectric constant,  $\rho$  electrical resistivity,  $\epsilon_r$  ( $\text{CaF}_2$ ) = 6.81). This is opposite to other insulating materials, e.g. quartz with  $\tau_0 \cong 400$  s; i.e. contrary to the electron-beam-induced charge behaviour of poorly conducting materials in the case of the cleaved surface of  $\text{CaF}_2$  during the slow scan period ( $t_f = 80$  s)  $\tau_0$  is much smaller than  $t_f$ . Consequently the surface charge density shows a locally oscillating behaviour and does not approach its maximum value which is given for  $\tau_0 \gg t_f$  [14].

Finally, the advantageous effect of an electrical retarding field realized by a grounded metallic grid conductively fixed on the cleaved surface (see Fig. 1b) is demonstrated by Fig. 6. Below  $E_p = 10$  keV within the meshes no precharging dose effect of charge accumulation during repeated slow scans with  $t_f = 80$  s disturbing the imaging of topographic details could be observed. Therefore, because of a presumably great loss of charge due to the relatively high electrical conductivity of the cleaved surface we assume the momentary maximum of the effective field strength – given by the effective surface voltage in the centre of the meshes and the half width of the single mesh – does not exceed  $4 \times 10^4$  V/cm for  $E_p = 10$  keV in this case.

### 3.2 The polished surface

The situation is completely different for the polished  $\text{CaF}_2$  surface. Usually, a damaged layer of a thickness of several hundred nm dependent on the polishing parameters is formed during the polishing process [15]. Therefore, we expect an extremely high concentration of

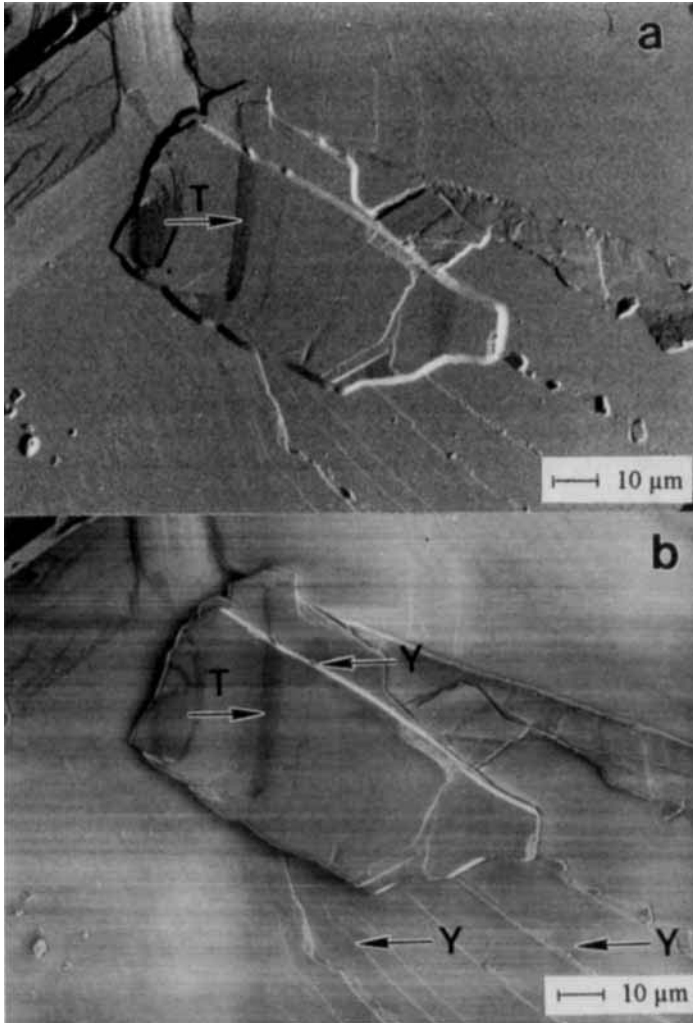


Fig. 5. Different electron trajectory-related contrast formation of the slow scan image of an uncoated cleavage face due to charge;  $E_p = 5$  keV. a) Backscattered electron mode (topography contrast), b) secondary electron mode (arrows T and Y see text)

trapped charges inherent in the damaged surface layer resulting in a spontaneous charge-up of the uncoated specimen area even for small beam energies. This usually means that it is impossible to inspect the uncoated polished crystal with respect to scratches, inclusions, abrasive spots, and also to local, not topographically determined, SE yield variations because its surface shows a pronounced effect of precharge dose and charge accumulation such that the electron probe cannot penetrate the solid surface.

Fig. 7 illustrates this different charge behaviour of polished and cleaved crystal surfaces of CaF<sub>2</sub>. On the uncoated polished surface contacted as shown in Fig. 1a an electrostatic potential area around the “implanted charge” of the electron probe can already be generated for a beam energy of  $E_p < 3$  keV in this case resulting in the SEM mirror effect of the

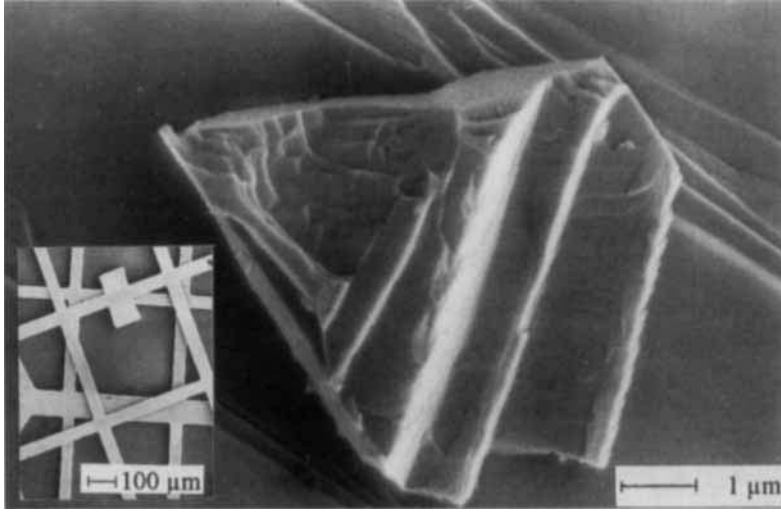


Fig. 6. Discharging effect of a grounded large-area metallic grid (see inset) conductively fixed on the centre of the uncoated cleavage face (cf. Fig. 1 b): within the openings of a size of  $500 \times 500 \mu\text{m}^2$  a high magnified SE slow scan imaging of small crystallites is obtained free of charge;  $E_p = 3 \text{ keV}$

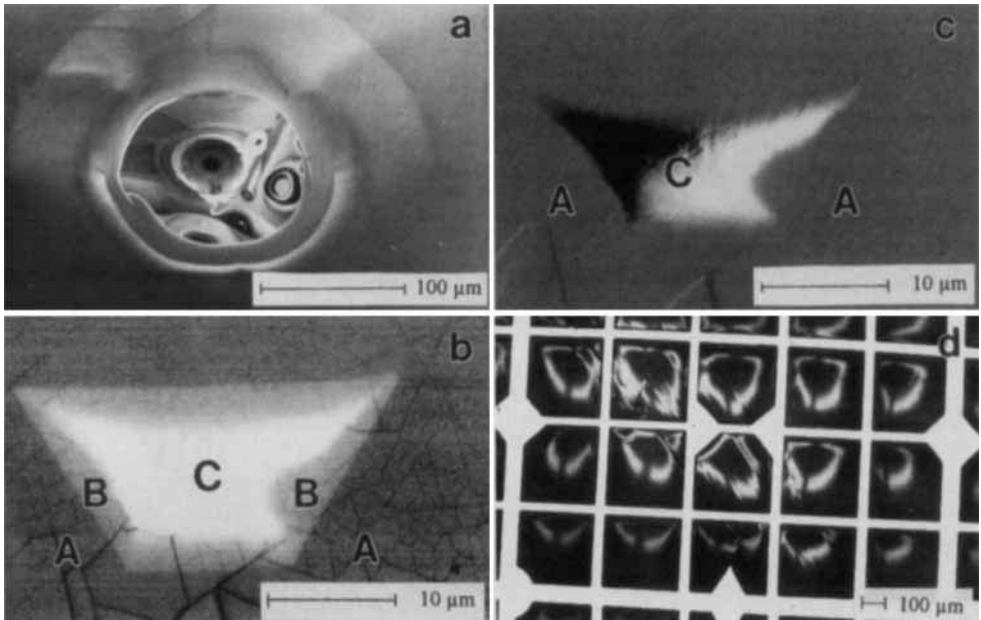


Fig. 7. Illustration of the different charge behaviour of both crystal surfaces: a) typical (slowly distorted) electron mirror micrograph of SEM components due to charge-up of the polished face, SE,  $E_p = 0.8 \text{ keV}$ . b) BE material contrast and c) BE topography contrast of a locally *uncoated* area of the carbon coated polished surface,  $E_p = 3.7 \text{ keV}$ . d) Retarding field effect of a metallic grid above the critical beam energy of the onset of charge-up, BE material contrast;  $E_p = 20 \text{ keV}$ , cleaved surface

charged surface [16]. For this aim, firstly, an equipotential surface is created for a beam energy of several keV. If then a beam energy of  $E_p \approx 1$  keV is applied, slightly distorted low-noise SE micrographs of details of the detector and pole piece arrangement of the microscope can easily be obtained (Fig. 7a). The charge *decay* takes about 15 min in this case, enough for many slow scans of  $t_f = 80$  s.

Strong charge accumulation on the uncoated polished surface surrounded by a grounded conducting film is also detectable by means of BE imaging (Fig. 7b and 7c). In this case the sum ( $S_1 + S_2$ ) of both signals of the SEM stereo detector as well as their difference

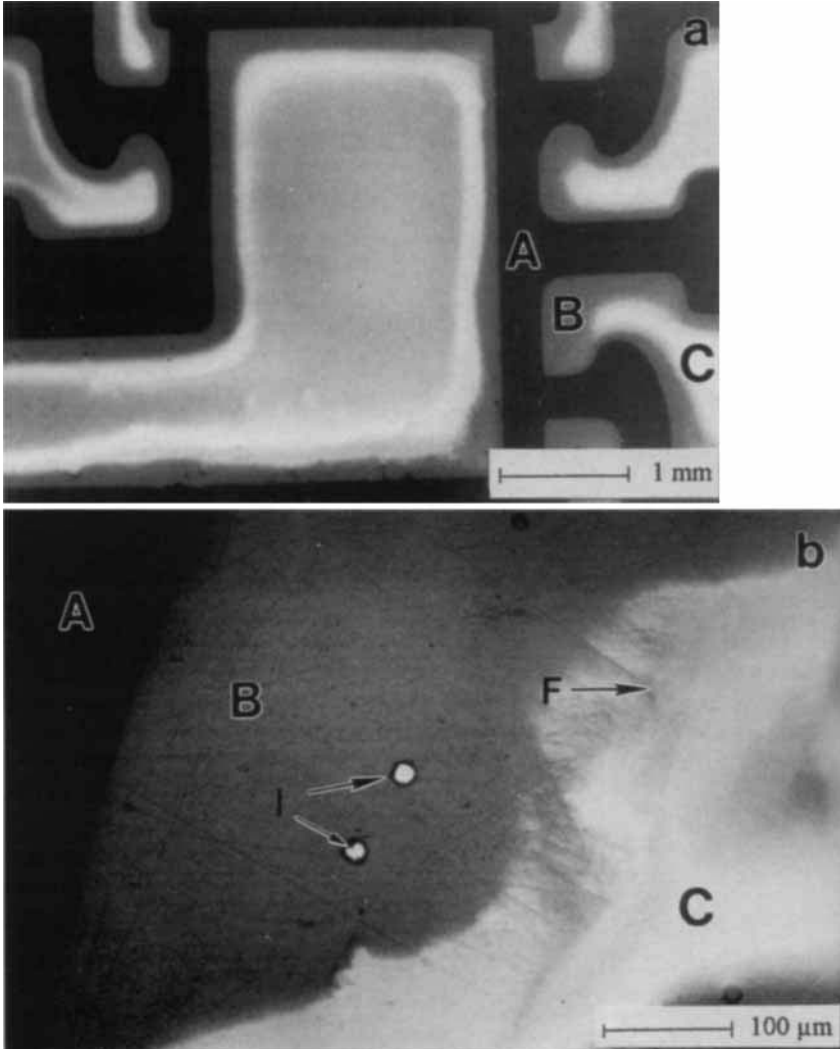


Fig. 8. Evidence of defects of the uncoated polished surface located in the deceleration field zone B between grounded electrical conducting paths A and the chargeable part C, SE,  $E_p = 2$  keV,  $\Phi = 0^\circ$ . a) Survey micrograph of the applied lithography (cf. Fig. 1c); b) an enlarged detail of a) showing two inhomogeneities (I) of area B

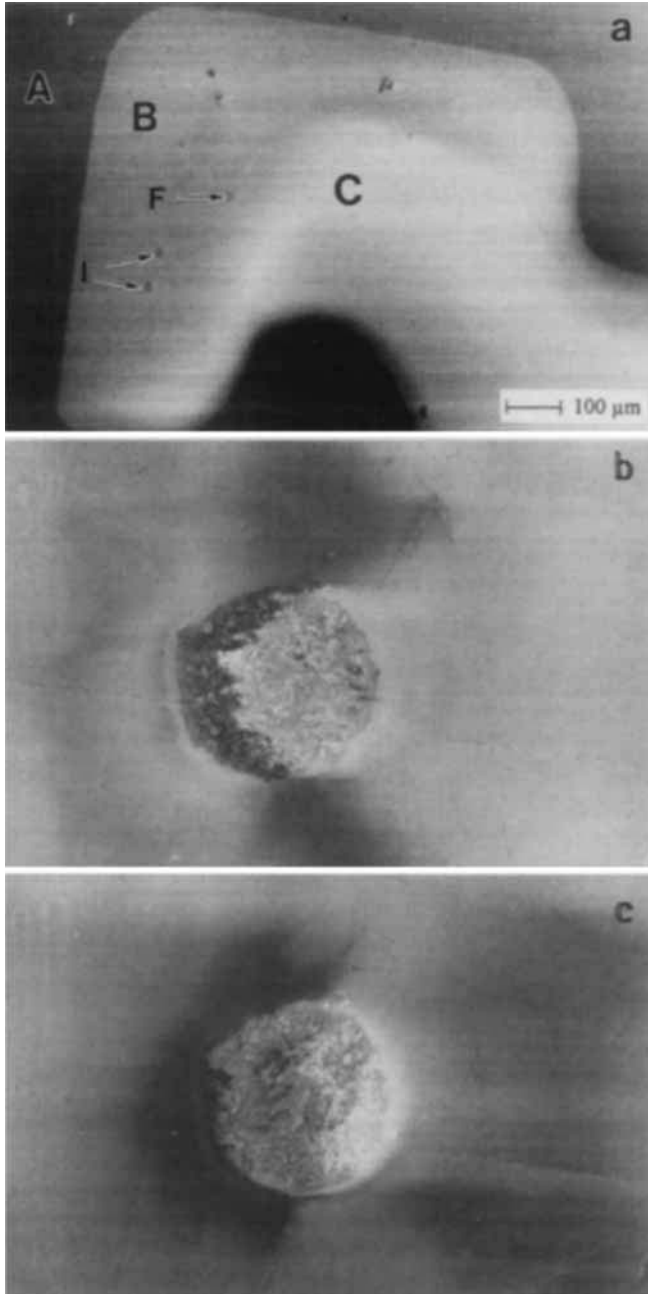


Fig. 9. Detailed inspection of the uncoated polished surface (cf. Fig. 8b). a) Charge reduction (area C) and contrast inversion (inhomogeneities I) due to specimen tilting ( $\Phi = 36^\circ$ ,  $E_p = 2$  keV), the border line B/C can sensitively be shifted through the inhomogeneity F by varying  $\Phi$  between b)  $\Phi = 21^\circ$  and c)  $23^\circ$ ,  $E_p = 4$  keV, SE

( $S_1 - S_2$ ) yield a distorted image due to the potential “blister” immediately formed after the first frame scan: In Fig. 7b the retarding field effect of the conducting surrounding A clearly enables to detect the real dimensions of the uncoated area B as material contrast. Due to the charge-induced repelling of the PE in the centre C a high “atomic number” contrast is simulated. On the contrary, the difference of the two signals simulates a topographically *convexly* formed spherical surface which really does *not* exist (Fig. 7c). Therefore, the BE topography mode shows a pronounced rise (dark) and falling edge (bright) contrast of the charged area C in this case totally suppressing the border line between coated A and uncoated B areas. This already happens for  $E_p < 5$  keV. To create similar charge patterns on the *cleavage face* of CaF<sub>2</sub> a much higher beam energy of  $E_p > 15$  keV is necessary. We obtained a very weak contrast by means of the same BE modes (Fig. 7d, material contrast) indicating a strongly increased surface charge leakage in this case.

To overcome the charge problem of the uncoated polished surface in selected areas conducting paths were prepared lithographically, Fig. 1c (schematically) and Fig. 8a (survey micrograph). Only if the area of interest is located within or nearby a lateral decelerating (retarding) field between grounded conducting paths (A) and the chargeable uncoated insulator area (C) SE micrographs without distortion by high SE yield can be obtained (Fig. 8b, area B). The potential distribution of the uncoated surface areas turns out to be stable in time if the system of the conducting paths is grounded and it is strongly floating if they are not grounded. It should be noted that on the polished crystal surface very different charge phenomena can arise, which can sensitively be distinguished during the low voltage SE imaging by varying solely the specimen tilt  $\Phi$  (i.e. the angle between the surface normal and the incident electron beam) for constant beam energy:

Local inhomogeneities (I) of the transition region B which are still clearly negatively charged for  $\Phi = 0^\circ$  (see Fig. 8b) exhibit a reversal in contrast for  $\Phi > 30^\circ$  (Fig. 9a). However, the charge of the extended type C area is only reduced and may not have changed sign in this case. Although disturbances on insulators inherent in charge-up can be eliminated by varying  $\Phi$  for fixed  $E_p$  compared with the cleaved surface, on the polished surface it is much more difficult to find imaging conditions *totally* free of charge over an extended area if the specimen tilt is changed. Due to the defect-related high sensitivity of charge-up of the polished surface in small areas (the input charge  $\sigma_i$  per unit picture element is  $\sim M^2$ ,  $M$  is the magnification [17]) on type C areas here we succeed to charge  $\mu\text{m}$  sized inhomogeneities very differently only by varying the tilt angle in steps of about  $\Delta\Phi = 2^\circ$  (Fig. 9b, c). These imaging conditions are stable in time.

#### 4. Conclusions

The great difference of the surface charge-up characteristics under electron beam irradiation of the uncoated cleaved and polished surface of CaF<sub>2</sub> single crystals directly evidences a relation between the density of surface defects due to preparation and the surface potential strongly influencing the SEM imaging conditions. Obviously, if one assumes that an insulator with a small number of defects would hardly be charged, the density of cleavage-induced surface defects may be essentially smaller than that introduced by the abrasive mechanical polishing procedure generating a regular mirror surface for primary electrons.

In spite of their different depth of information and contrast mechanisms SE and BE signals turn out to be equally suitable for the detection of this difference of the charge behaviour for both surfaces. Unavoidable surface contaminations like carbon, oxygen, and moisture do not cover this fundamental difference which after selective etching experiments on both surfaces could possibly be interpreted in more detail as resulting from strongly different density and distribution of lattice defects.

In future, the results given here could be supported by a careful measurement of the electrical *surface* conductivity (especially on terraces free of steps in the case of a cleavage face) and will be compared with SEM charge phenomena induced by laser pulses of the same material below and above the observable damage threshold. Up to now only data for the *bulk* conductivity of CaF<sub>2</sub> or for CaF<sub>2</sub> *films* on semiconducting substrates [18] are known. Polished surfaces of CaF<sub>2</sub> that have a great importance for optical components could also be changed in their charge behaviour by removal of a thin polycrystalline surface layer by means of a selective *chemical* polishing which has been reported for other fluoride crystals [19] but up to now not for CaF<sub>2</sub> to our knowledge. To study the effect of a successively diminished influence of mechanical polish damage on the formation of surface charge detectable by SEM measurements of the surface potential could directly be correlated with a microtexture analysis of the same specimen area by means of the so-called SEM "orientation mapping" of backscattered Kikuchi patterns [20].

### Acknowledgements

Continued support by E. Matthias is gratefully acknowledged. This work was supported by Deutsche Forschungsgemeinschaft, Sfb 337.

### References

- [1] M. KOTERA, T. SAYAMA, and H. SUGA, Proc. 11th Internat. Congr. Electron Microscopy, Tokyo 1986 (pp. 413–414).
- [2] J. P. VIGOROUX, J. P. DURAUD, A. LE MOEL, and C. LE GRESSUS, J. appl. Phys. **57**, 5139 (1985).
- [3] J. T. DICKINSON, L. C. JENSEN, R. L. WEBB, M. L. DAWES, and S. C. LANGFORD, J. appl. Phys. **74**, 3758 (1993).
- [4] T. S. SUDARSHAN and J. WANG, IEEE Trans. Electrical Insulation **27**, 1127 (1992).
- [5] J. CAZAUX and C. LE GRESSUS, Scanning Microscopy **5**, 17 (1991).
- [6] H. J. FITTING, H. GLAEFEKE, W. WILD, M. FRANKE, and W. MÜLLER, Exper. Tech. Phys. **27**, 13 (1979).
- [7] H. BRUCH, P. GÖRLICH, H. KARRAS, and R. LEHMANN, phys. stat. sol. **4**, 685 (1964).
- [8] C. L. STRECKER, W. E. MODDEMANN, and J. T. GRANT, J. appl. Phys. **52**, 6921 (1981).
- [9] S. BAUNACK and A. ZEHE, Surface Sci. **225**, 292 (1990).
- [10] L. REIMER, R. GOLLA, M. BÖNGELER, B. KÄSSENS, and R. SENKEL, Optik **92**, 14 (1992).
- [11] P. J. MÖLLER and J. P. HE, Nuclear Instrum. and Methods **B17**, 137 (1986).
- [12] M. SVANTNER and E. MARIANI, Kristall und Technik **13**, 1431 (1978).
- [13] D. K. DAVIES, Static Electrification, IPPS Conf. Ser. No. **4A**, Inst. Phys. and Phys. Soc., London 1967 (p. 29).
- [14] R. D. VAN VELD and T. J. SHAFFNER, SEM/1971, AMF O'Hare, Chicago (p. 17 to 24).
- [15] H. DUNKEN and U. KRILTZ, Exper. Tech. Phys. **39**, 71 (1991).
- [16] J. P. VIGOROUX, O. LEE-DEACON, C. LE GRESSUS, C. JURET, and C. BOIZIAU, IEEE Trans. Electrical Insulation **18**, 287 (1983).
- [17] T. KODAMA and Y. UCHIKAWA, J. Electron Microscopy **41**, 65 (1992).
- [18] J. G. COOK, G. H. YOUSEFI, S. R. DAS, and D. F. MITCHELL, Thin Solid Films **217**, 87 (1992).
- [19] C. A. BROOKES and J. E. MORGAN, J. Mater. Sci. **12**, 2542 (1977).
- [20] R. A. SCHWARZER, Mater. Sci. Forum **157/162**, 187 (1992).